Proteomics

DOI: 10.1002/ange.201309135

Organelle-Specific Activity-Based Protein Profiling in Living Cells**

*Susan D. Wiedner, Lindsey N. Anderson, Natalie C. Sadler, William B. Chrisler, Vamsi K. Kodali, Richard D. Smith, and Aaron T. Wright**

Abstract: *A multimodal activity-based probe for targeting acidic organelles was developed to measure subcellular native enzymatic activity in cells by fluorescence microscopy and mass spectrometry. A cathepsin-reactive warhead conjugated to a weakly basic amine and a clickable alkyne, for subsequent appendage of a fluorophore or biotin reporter tag, accumulated in lysosomes as observed by structured illumination microscopy (SIM) in J774 mouse macrophage cells. Analysis of in vivo labeled J774 cells by mass spectrometry showed that the probe was very selective for cathepsins B and Z, two lysosomal cysteine proteases. Analysis of starvation-induced autophagy, a catabolic pathway involving lysosomes, showed a large increase in the number of tagged proteins and an increase in cathepsin activity. The organelle-targeting of activity-based probes holds great promise for the characterization of enzyme activities in the myriad diseases linked to specific subcellular locations, particularly the lysosome.*

Activity-Based Protein Profiling (ABPP) utilizes targeted chemical probes to determine enzyme activities in vitro, in situ, or in vivo.[1] Employing probe derivatives that contain an azide or alkyne moiety permits multiple applications of ABPP, such as fluorescence microscopy and mass spectrometry (MS), by direct attachment of reporting groups through copper-catalyzed azide–alkyne cycloadditions (CuAAC).[2] Small probe size increases cell permeability, thereby allowing interrogation of the native proteome within intact cells. The use of ABPP to irreversibly bind shared catalytic features of soluble enzyme families within a defined organelle population is an exceptional challenge for chemoproteomics.[3] Organelle proteomics is plagued by difficulties in distinguishing true resident proteins from copurifying contaminant proteins, and cellular disruption for organelle isolation potentially interferes with native enzymatic activity.[4] We thus endeavored to analyze specific active enzyme populations in defined organelles within live cells by using cell-permeable organelle-directed activity-based probes (ABP).

We envisioned an acidotropic ABP that would accumulate in acidic organelles for the interrogation of resident enzyme activity. High molecular weight probes containing fluorophores and/or enrichment tags are known, but they require cell penetrating peptides or receptor motifs, in addition to long labeling times, in order to enter live cells and accumulate.[5] Smaller ABPs can reach their enzyme target quickly, but any organelle accumulation is due to enzyme localization rather than defined probe properties.[2b,6] Our envisioned ABP requires a moiety with specific physicochemical properties[7] and an alkyne for CuAAC-mediated conjugation of a fluorophore or enrichment tag.

As a proof of concept, we designed a lysosome-targeting ABP. Lysosomes are ubiquitous in mammalian cells, important for cell homeostasis, and play a role in cancer, Alzheimer's disease, and numerous orphan diseases.[8] Lysosomes are acidic organelles (pH value < 5) that contain at least 60 soluble hydrolase enzymes. Lysosomal proteomics is increasingly important for the study of lysosome-associated diseases and the discovery of novel enzymes.[8] Lysosomes are targeted by weakly basic amines and lipophilic moieties, which accumulate in acidic environments owing to passive diffusion of a neutral species across the membrane into an acidic milieu where the weak base is protonated, thereby preventing diffusion back across the membrane.[9]

We targeted acidic organelles by incorporating readily available 3-(2,4-dinitroanilino)-3′-amino-*N*-methyldipropylamine (DAMP) into an ABP (Figure 1). DAMP is known to rapidly accumulate in acidic organelles owing to its primary amine and pK_a value of approximately 10.[10] Furthermore, the DAMP primary amine provides a handle to append 1) an alkyne for CuAAC,[11] and 2) a broadly reactive inhibitor of papain cysteine protease, ethyl succinate epoxide, which is extensively used for labeling cathepsins.[2b,5,6,11] The synthesis of organelle-targeting DAMP epoxide probes (DEX-1 and DEX-2) is described in the Supporting Information (Figure 1

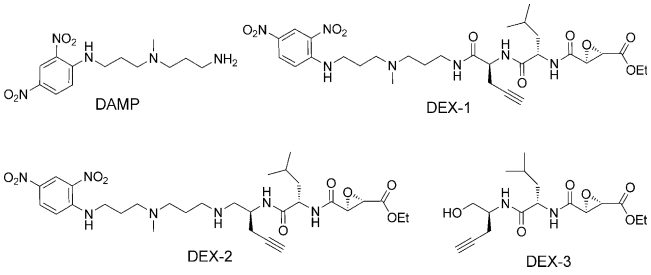

Figure 1. DAMP-derived lysosome-targeting activity-based probes.

[*] Dr. S. D. Wiedner, L. N. Anderson, N. C. Sadler, W. B. Chrisler, V. K. Kodali, Dr. R. D. Smith, Dr. A. T. Wright
Biological Sciences Division, Pacific Northwest National Laboratory
902 Battelle Blvd, Richland, WA 99352 (USA)
E-mail: aaron.wright@pnnl.gov

[**] This work was supported in part by the Laboratory Directed Research and Development Program at PNNL, a multiprogram national laboratory operated by Battelle for the U.S. DOE under Contract DE-AC05-76L01830, and by the NIH NIGMS (8 P41 GM103493-11). S.D.W. was supported by the PNNL Linus Pauling Distinguished Postdoctoral Fellowship. Work was performed in the Environmental Molecular Sciences Laboratory, a US DOE-BER national scientific user facility at PNNL. This work used instrumentation and capabilities developed under support from the NIH (8 P41 GM103493-11) and the DOE-BER.

Supporting information for this article is available on the WWW under http://dx.doi.org/10.1002/anie.201309135.

and Figures S1 and S2 in the Supporting Information). An ABP lacking DAMP (DEX-3) was synthesized as a weak-acid negative control (Figure 1 and Figure S2).[9] We suspected that disruption of an intramolecular hydrogen bond between the basic amines of DAMP by incorporating the amide of DEX-1 would prevent efficient accumulation in acidic organelles; therefore, we synthesized the amine derivative DEX-2.

We applied our suite of organelle-targeting probes to A549 human epithelial cells and J774 mouse macrophage cells (Figure 2). Imaging revealed DEX-2 accumulation in punctate vesicles throughout the A549 and J774 cells, while DEX-3 and DEX-1 gave diffuse cell labeling (Figure 2). The more basic DEX-2 accumulates in punctate vesicles quickly and permanently (Figure S3), with little cytosolic labeling. All ABPs react with similar nucleophilic proteases in A549 global cell lysate (Figure S4A); additionally, comparison of in vivo J774 labeling shows that DEX-1 and DEX-2 have similar intracellular targets except for two intense bands of low molecular weight (MW, <30 kDa, Figure S4B). Selective labeling of these low MW proteins and accumulation of DEX-2 is thus dependent on the basic amine.

The accumulation of DEX-2 is dependent on the acidic environment of the target organelle and the activity of the target enzyme. Pretreatment of J774 with excess NH_4Cl, known to neutralize acidic environments, reduced the labeling intensity of the punctate vesicles (Figure S5). Pretreatment of the cells with iodoacetamide (IAM) or ethyl (*2S*,3*S*)-oxirane dicarboxylate also reduced the labeling intensity (Figure S5). The fluorescence-imaging experiments are consistent with gel-based analysis; pretreatment of J774 cells with NH_4Cl and a slight excess of the cathepsin inhibitor E-64d suppresses labeling of the bands at 52 kDa, 31 kDa (*), and 27 kDa (*), thus suggesting that these proteins are cathepsins and that labeling is dependent on the acidic environment (Figure 3). The aspartyl protease inhibitor pepstatin A did not suppress labeling. DEX-2 labels purified cathepsin B and J774 proteins in a dose-dependent manner (Figure S6). Notably, the intense band at approximately 40 kDa appears to be the result of CuAAC (Figure S7).

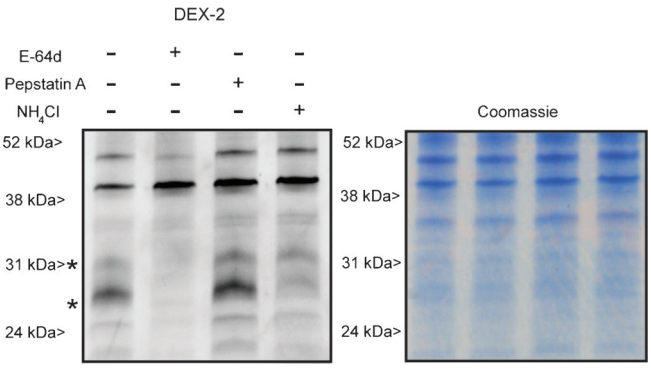

Figure 3. SDS-PAGE fluorescence imaging of DEX-2 labeled proteins in J774 cells following in vivo pretreatment with E-64d (58 μM), pepstatin A (58 μM), or NH_4Cl (30 mM) and then labeled with DEX-2 (37 μM). The Coomassie protein stain (right-hand image) shows equivalent protein loading of gel lanes. LC–MS analysis of J774 cells labeled in vivo with DEX-2 confirms labeling of CatB (28 kDa) and CatZ (27 kDa), which are indicated by asterisks.

To identify the site of DEX-2 accumulation, J774 cells treated with DEX-2 were immunostained for LAMP1, a lysosome-membrane marker (Figure 4A). Confocal laser scanning microscopy showed partial colocalization of DEX-2 with LAMP1 (Pearson's correlation coefficient (PCC) = 0.595 ± 0.082, $M_1 = 0.919 \pm 0.026$, $M_2 = 0.958 \pm 0.014$;[12] Figure 4A). In fact it appears that a LAMP1-positive membrane ring encircles the fluorescence signal of DEX-2 (arrows, Figure 4A).[13] This encapsulation of the probe signal by LAMP1 can be visualized at a resolution below the diffraction limit of light (<200 nm) by using super-resolution structured illumination microscopy (SIM; Figure 4B).[14] Z-stack imaging revealed that this phenomenon is found all the way through the vesicle (Figure 4B and Videos S1 and S2 in the Supporting Information), thus demonstrating that the probe is confined within the lysosome.

We performed high resolution LC–MS/MS[22] analysis of J774 cells treated with DEX-2 to characterize enzyme targets under two growth conditions. No-probe DMSO controls were run in parallel to account for background labeling. We identified six proteins in healthy J774 cells (Table S1 in the Supporting Information). Cathepsins B and Z were the most abundant proteins measured. J774 cells were also labeled under starvation-induced autophagy to determine whether lysosome-targeted DEX-2 could report on enzyme activity changes during stress (Figure S8). Autophagy, the digestion and recycling of cellular components such as organelles and intracellular proteins,[15] is important for cell homeostasis and response to stress and has been identified as playing a role in cancer and

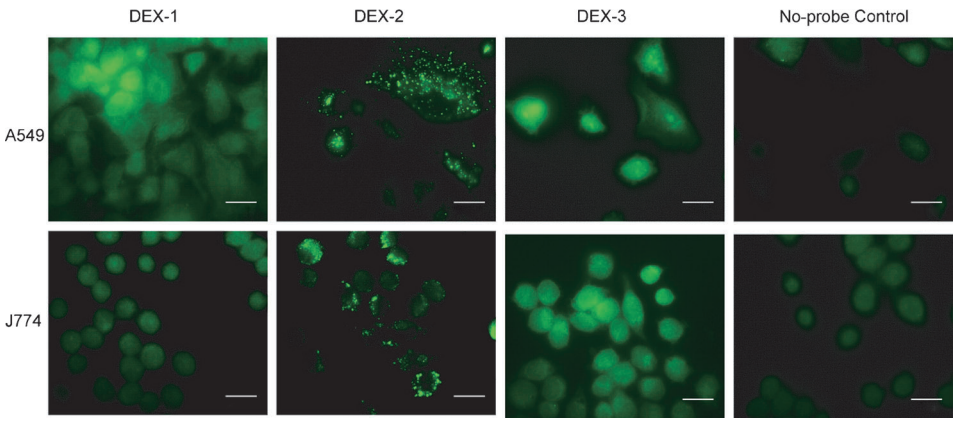

Figure 2. A549 and J774 cells were incubated with the DEX probes (10 μM and 2 μM, respectively, 1 h), fixed, and conjugated to AlexaFluor 488 through CuAAC. DEX-2 gives punctate vesicle staining in both cell lines. DEX-3 and DEX-1 give diffuse labeling throughout the cell. The no-probe control corresponds to DMSO treatment followed by CuAAC with the fluorophore. Scale bars: 20 μm.

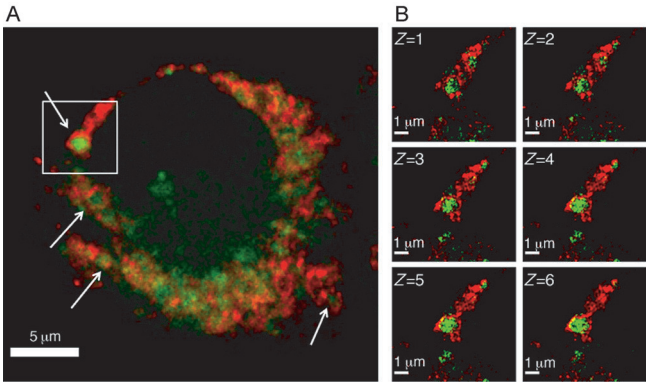

Figure 4. Colocalization of DEX-2 (green) with LAMP1 (red) in J774 cells. The J774 cells were treated with DEX-2 (2 μM) for 1 h. The cells were fixed and the probe was conjugated to AlexaFluor 488. The lysosomes were stained by immunofluorescence with anti-LAMP1, a goat anti-rabbit IgG–Alexafluor 647 antibody. A) Confocal laser scanning microscopy shows the green DEX-2 signal surrounded by the red LAMP1 signal (indicated by arrows). B) The boxed region of the confocal image was analyzed further by enhanced-resolution SIM. Shown are the vertical Z-plane images. Running from the top of the compartment ($Z=1$) to the middle of the compartment ($Z=6$); each image represents a 110 nm step.

Alzheimer's disease.[16] Studies have shown that the expression and/or efficiency of hydrolytic enzymes can change during autophagy.[17] Furthermore, DAMP accumulates in autolysosomes, a fused lysosome–autophagosome in which degradation occurs.[18] By using the same data-filtering criteria, DEX-2 labeled 44 proteins during autophagy (Table S1). 17 of the 44 proteins have previously been observed in autophagosomes under nitrogen-starvation-induced autophagy in human MCF7-eGFP-LC cells by stable isotope labeling by amino acids in cell culture (SILAC) and protein correlation profiling analysis.[19]

Autophagy constitutes degradation of cellular proteins and organelles in autolysosomes. Consistent with this, DEX-2-labeled proteins in autophagic cells come from a range of cellular locales including the cytosol, mitochondria, actin cytoskeleton, and endoplasmic reticulum. Previously, a global SILAC proteomics analysis of amino acid starved MCF7-eGFP-LC3 cell lysate found that proteins associated with these locations decreased in abundance to different extents over a 36 h period.[20] Our observation of these proteins within acidic organelles after only 1 h of starvation showcases the sensitivity of our organelle-targeting ABP method. The loss in the selectivity of DEX-2 for cysteine proteases observed in autophagic cells is likely due to nucleophilic-residue exposure resulting from partial degradation of these proteins during autophagy.

We observed that enzyme activity increases during autophagy. Cathepsins B and Z showed a moderate increase of 1.6-fold (p-value < 0.05). Previous studies show that short-term starvation and amino acid deprivation induce proteolysis.[13,17b,21] Furthermore, in mouse liver, cathepsin B activity initially decreases but then increases over 68 h of starvation.[21] These enzyme activity assays were performed on liver homogenate and may not accurately portray enzyme activity in the native cellular environment. The small activity increase we measured for the cathepsins correlates with the very short starvation interval used to induce autophagy in this study and the transient nature of autolysosomes in autophagic flux. It also demonstrates that Cathepsin B enzymatic activity is variable and contingent upon cellular conditions.

In conclusion, we developed a multimodal organelle-targeting ABP that rapidly accumulates in punctate vesicles owing to the physicochemical characteristics of a weakly basic amine. Through super-resolution SIM, we provide evidence that these punctate vesicles are lysosomes. The probe was also used to measure enzyme activity changes upon the induction of autophagy in macrophage cells. The direction of an ABP to specific organelles through its physicochemical properties should be applicable to other organelles. Additionally, switching the electrophilic warhead of a defined organelle-targeting ABP would allow the targeting of other resident enzyme families. We believe this approach could fuse organelle and activity-based proteomics and that it could be widely applicable for the analysis of biological systems.

Received: October 18, 2013
Revised: November 26, 2013
Published online: February 6, 2014

Keywords: activity-based probes · fluorescence microscopy · lysosome · mass spectrometry · proteomics

[1] N. Li, H. S. Overkleeft, B. I. Florea, *Curr. Opin. Chem. Biol.* **2012**, *16*, 227–233.
[2] a) A. E. Speers, B. F. Cravatt, *Chem. Biol.* **2004**, *11*, 535–546; b) H. C. Hang, J. Loureiro, E. Spooner, A. W. M. van der Velden, Y.-M. Kim, A. M. Pollington, R. Maehr, M. N. Starnbach, H. L. Ploegh, *ACS Chem. Biol.* **2006**, *1*, 713–723.
[3] P.-Y. Yang, K. Liu, C. Zhang, G. Y. J. Chen, Y. Shen, M. H. Ngai, M. J. Lear, S. Q. Yao, *Chem. Asian J.* **2011**, *6*, 2762–2775.
[4] Y. H. Lee, H. T. Tan, M. C. M. Chung, *Proteomics* **2010**, *10*, 3935–3956.
[5] a) U. Hillaert, M. Verdoes, B. I. Florea, A. Saragliadis, K. L. L. Habets, J. Kuiper, S. Van Calenbergh, F. Ossendorp, G. A. van der Marel, C. Driessen, H. S. Overkleeft, *Angew. Chem.* **2009**, *121*, 1657–1660; *Angew. Chem. Int. Ed.* **2009**, *48*, 1629–1632; b) F. Fan, S. Nie, E. B. Dammer, D. M. Duong, D. Pan, L. Ping, L. Zhai, J. Wu, X. Hong, L. Qin, P. Xu, Y.-H. Zhang, *J. Proteome Res.* **2012**, *11*, 5763–5772.
[6] a) D. Greenbaum, A. Baruch, L. Hayrapetian, Z. Darula, A. Burlingame, K. F. Medzihradszky, M. Bogyo, *Mol. Cell. Proteomics* **2002**, *1*, 60–68; b) W. W. Kallemeijn, K.-Y. Li, M. D. Witte, A. R. A. Marques, J. Aten, S. Scheij, J. Jiang, L. I. Willems, T. M. Voorn-Brouwer, C. P. A. A. van Roomen, R. Ottenhoff, R. G. Boot, H. van den Elst, M. T. C. Walvoort, B. I. Florea, J. D. C. Codée, G. A. van der Marel, J. M. F. G. Aerts, H. S. Overkleeft, *Angew. Chem.* **2012**, *124*, 12697–12701; *Angew. Chem. Int. Ed.* **2012**, *51*, 12529–12533.
[7] a) J. Kornhuber, P. Tripal, M. Reichel, C. Mühle, C. Rhein, M. Muehlbacher, T. W. Groemer, E. Gulbins, *Cell. Physiol. Biochem.* **2010**, *20*, 9–20; b) Y. Kurishita, T. Kohira, A. Ojida, I. Hamachi, *J. Am. Chem. Soc.* **2012**, *134*, 18779–18789.
[8] T. Lübke, P. Lobel, D. E. Sleat, *Biochim. Biophys. Acta Mol. Cell Res.* **2009**, *1793*, 625–635.
[9] C. De Duve, T. De Barsy, B. Poole, A. Trouet, P. Tulkens, F. Van Hoof, *Biochem. Pharmacol.* **1974**, *23*, 2495–2531.

[10] R. G. Anderson, J. R. Falck, J. L. Goldstein, M. S. Brown, *Proc. Natl. Acad. Sci. USA* **1984**, *81*, 4838 – 4842.
[11] D. Greenbaum, K. F. Medzihradszky, A. Burlingame, M. Bogyo, *Chem. Biol.* **2000**, *7*, 569 – 581.
[12] S. V. Costes, D. Daelemans, E. H. Cho, Z. Dobbin, G. Pavlakis, S. Lockett, *Biophys. J.* **2004**, *86*, 3993 – 4003.
[13] N. Mizushima, A. Yamamoto, M. Matsui, T. Yoshimori, Y. Ohsumi, *Mol. Biol. Cell* **2004**, *15*, 1101 – 1111.
[14] I. Davis, *Biochem. Soc. Trans.* **2009**, *37*, 1042 – 1044.
[15] V. Kaminskyy, B. Zhivotovsky, *Biochim. Biophys. Acta Proteins Proteomics* **2012**, *1824*, 44 – 50.
[16] B. Levine, G. Kroemer, *Cell* **2008**, *132*, 27 – 42.
[17] a) D. Muno, N. Sutoh, T. Watanabe, Y. Uchiyama, E. Kominami, *Eur. J. Biochem.* **1990**, *191*, 91 – 98; b) G. Fuertes, J. J. Martín De Llano, A. Villarroya, A. J. Rivett, E. Knecht, *Biochem. J.* **2003**, *375*, 75 – 86; c) H.-M. Ni, A. Bockus, A. L. Wozniak, K. Jones, S. Weinman, X.-M. Yin, W.-X. Ding, *Autophagy* **2011**, *7*, 188 – 204.
[18] W. A. Dunn, *J. Cell Biol.* **1990**, *110*, 1935 – 1945.
[19] J. Dengjel, M. Høyer-Hansen, M. O. Nielsen, T. Eisenberg, L. M. Harder, S. Schandorff, T. Farkas, T. Kirkegaard, A. C. Becker, S. Schroeder, K. Vanselow, E. Lundberg, M. M. Nielsen, A. R. Kristensen, V. Akimov, J. Bunkenborg, F. Madeo, M. Jäättelä, J. S. Andersen, *Mol. Cell. Proteomics* **2012**, *11*, M111.014035.
[20] A. R. Kristensen, S. Schandorff, M. Høyer-Hansen, M. O. Nielsen, M. Jäättelä, J. Dengjel, J. S. Andersen, *Mol. Cell. Proteomics* **2008**, *7*, 2419 – 2428.
[21] T. Inubushi, M. Shikiji, K. Endo, H. Kakegawa, Y. Kishino, N. Katunuma, *Biol. Chem.* **1996**, *377*, 539 – 542.
[22] MS/MS spectra for all DEX-2 studies have been uploaded into PeptideAtlas under dataset identifier PASS00302; http://www.peptideatlas.org/PASS/PASS00302.